Power Electronic Systems
Laboratory

Proceedings of the IEEE Energy Conversion Congress and Exposition (ECCE USA 2012), Raleigh, USA, September 16-20, 2012

Novel Signal Injection Methods for High-Speed Self-Sensing Electrical Drives

A. Tüysüz,
M. Schöni,
J.W. Kolar

Eidgenössische Technische Hochschule Zürich
Swiss Federal Institute of Technology Zurich

Novel Signal Injection Methods for High Speed Self-Sensing Electrical Drives

A. Tüysüz, M. Schöni, and J.W. Kolar
Power Electronic Systems Laboratory, ETH Zurich
CH-8092 Zurich, Switzerland
tuysuz@lem.ee.ethz.ch

Abstract— **This paper proposes a novel self-sensing method for high speed electrical drives. Signal injection, measurement, filtering and demodulation stages are built in dedicated hardware, reducing the computational effort for the signal processor and removing any need to modify the drive inverter operation. Differential measurements make this method applicable for even very low saliency machines such as slotless permanent magnet machines. Different variations of the proposed method are explained on two different machine examples. Experimental results verify the applicability of the proposed method.**

I. Introduction

Increasing the speed of an electrical machine decreases its volume and weight for a given power rating, which is a significant advantage in applications such as generators/starters for micro gas turbines, turbo compressors, micro spindles and dental/medical drills [1]. High speed electrical drives have been a popular research topic recently, exactly for this reason. Several high speed motors with speeds exceeding 100 000 rpm and power levels ranging from 100 W up to a few kWs have been dealt with in the literature [2]. The preferred motor topology for those applications is the slotless Permanent Magnet (PM) machine, as demonstrated in [3] and [4]. However, the interest in high speed drives has led to the investigation of different machine topologies as well. The lateral stator motor concept is introduced in [2] for micro drilling and milling applications, where the electrical machine needs to fit into confined spaces around the tool head.

Rotor position information is needed for a high performance operation of PM machines. Position sensors such as Hall Effect sensors can be used to obtain this information; however, they generally increase the cost and decrease the reliability of the drive system. Furthermore, they require additional space, which is in conflict with the miniaturization trend mentioned above. Therefore, self-sensing drives (drives without additional position sensors) are receiving increasing attention in the high speed area as well as electrical drives in general.

Several self-sensing approaches are described in literature, and they can be divided into two groups: approaches using the Back ElectroMotive Force (EMF) induced by the machine [3], and approaches tracking the machine impedance which depends on the rotor position [5]. As the back EMF gets harder to measure at low speeds and disappears at standstill, the first group of approaches is not operational in the full speed range, and as a result not considered any further in this paper.

In [6], the rotor position is measured by applying short voltage pulses to the machine in different space vector directions and measuring their current responses. This can be done either by interrupting the drive power to the machine and applying the voltage pulses for a short time interval [7], or by integrating the measurement pulses into the drive Pulse Width Modulation (PWM) [8]. The former method leads to torque distortions, acoustic noise, high current ripple and consequently high copper losses, whereas the latter requires complicated modifications of the PWM pattern, which means additional computational effort for the Digital Signal Processor (DSP). This becomes a severe problem with high speed drives having high fundamental and therefore high switching frequencies.

Another method of tracking the rotor position dependent impedance of the machine is by injecting a carrier frequency signal (generally a voltage) into the machine and extracting rotor position information from the phase or amplitude of its response (generally a current) [9]. Normally, the carrier frequency is selected significantly higher than the fundamental frequency of the drive current, and superimposed to the fundamental frequency by using the drive inverter. Compared to the short voltage pulses, this method has the advantages that it does not require the modification of the PWM patterns, additional di/dt sensors or oversampling of the current [10]. However, the complicated digital filtering and demodulation of the carrier frequency response in the DSP limits the practical application of this method to high speed drives. Furthermore, superimposing a significantly higher carrier frequency to the fundamental drive current may push the inverter switching frequency beyond practical limits.

An additional challenge for full speed range self-sensing control of high speed drives is the extremely low saliency of the slotless PM machines. The symmetrical construction of the machine and the lack of saturation in the iron core lead to an extremely weak dependency of the machine impedance on the rotor position. Either when using voltage pulses or carrier frequency signal injection, a high voltage needs to be applied to the machine for practical current sensors to be able to detect the small changes in the current response. This results in additional losses both in the machine and in the inverter.

In this paper, a new method for the full speed range self-sensing operation of high speed drives is proposed. First, the carrier frequency signal is injected into the machine using an additional low cost injection circuit. Decoupling the signal injection from the drive inverter removes the need for any modification of the PWM patterns or increasing the switching frequency. Differential measurements are used for detecting even weak changes in machine impedance with high accuracy. Finally, the filtering and demodulation are constructed in hardware, avoiding any additional computational effort for the DSP.

The proposed concept is explained using two examples; a lateral stator machine and a slotless PM machine.

II. Case I: Lateral Stator Machine

A. The Lateral Stator Machine

In an earlier work, the lateral stator machine topology (Figure 1) was suggested for direct drive micro spindle applications with space restrictions. Its design and construction are discussed in detail in [2] and [11], respectively. The self-sensing scheme presented in this paper is explained on this kind of machine first.

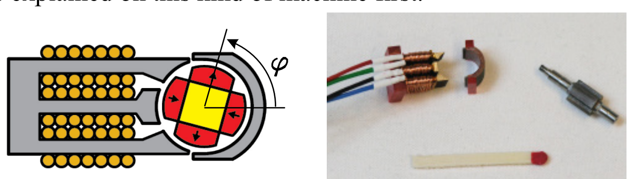

(a) (b)

Figure 1. Lateral stator machine. (a) Conceptual drawing. φ denotes the rotor position. Stator (gray), permanent magnets (red), rotor shaft (yellow), windings (orange). (b) Photo of the prototype.

B. Signal Injection and Differential Voltage Measurement

Figure 2 shows the key components of the self-sensing drive. A space vector modulation operated standard three phase two level inverter feeds power to the machine through an LCL sinus filter which limits the harmonics applied to the machine. A high frequency voltage (either sinusoidal or rectangular) is generated independent of the inverter and applied between the star point and one terminal of the machine. The high frequency current flows through one phase of the machine only; and completes its path (in red) through the capacitor C_{inj}. A voltage measurement is taken between the other two phases of the machine, and after filtering and demodulation stages, a signal containing the useful rotor position information is fed to the Analog-to-Digital Converter (ADC) of the DSP.

A high frequency current i_{inj} injected into phase B of the machine induces voltages u_{A} and u_{C} in A and C phases of the machine respectively:

$$i_{\text{inj}} = \hat{\imath}_{\text{inj}} \sin(\omega_{\text{inj}} t), \qquad (1)$$

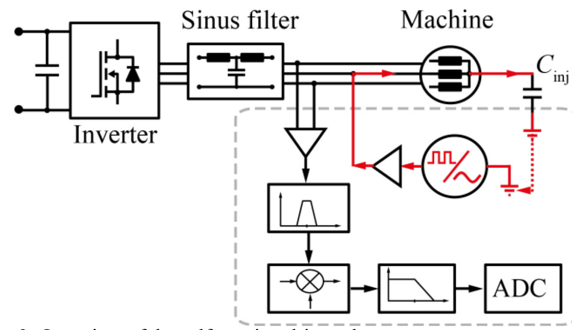

Figure 2. Overview of the self-sensing drive scheme.

$$u_A = L_{BA} \frac{di_B}{dt} = L_{BA} \cdot \omega_{inj} \cdot \hat{\imath}_{inj}\ cos(\omega_{inj} t), \qquad (2)$$

$$u_{\text{C}} = L_{\text{BC}} \frac{di_{\text{B}}}{dt} = L_{\text{BC}} \cdot \omega_{\text{inj}} \cdot \hat{\imath}_{\text{inj}}\ \cos(\omega_{\text{inj}} t), \qquad (3)$$

where L_{BA} and L_{BC} are the mutual inductances.

A differential voltage measurement gives the difference of the induced voltages as

$$u_{\text{AC}} = (L_{\text{BA}} - L_{\text{BC}}) \cdot 2\pi f_{\text{inj}} \cdot \hat{\imath}_{\text{inj}}\ \cos(\omega_{\text{inj}} t), \qquad (4)$$

where f_{inj} is the injection frequency.

Figure 3 (a) shows that for the lateral stator machine, the mutual inductances L_{BA} and L_{BC} depend strongly on the rotor position; hence the lateral stator machine is not a low saliency machine. However, it can be seen from (4) and Figure 3 (b) that, with a differential measurement, the full range of the ADC can be utilized for rotor position sensing. This is an important step towards achieving practical full speed range self-sensing drives with very low saliency machines.

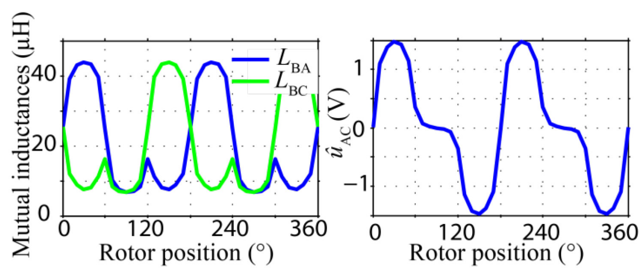

(a) (b)

Figure 3. Finite element analysis results showing (a) the mutual inductances, (b) peak value of the differential voltage response for sinusoidal current injection with f_{inj}=1.282 MHz, $\hat{\imath}_{\text{inj}}$ = 5 mA. x-axis shows rotor's position in electrical degrees.

As it can be seen in Figure 3, $\hat{u}_{\text{AC}}$, which contains rotor position information, goes flat for some rotor positions. This is caused by the machine geometry and it decreases the sensitivity of the position sensing. To overcome this problem, the current is injected to the machine through a resonant tank (Figure 4), whose resonant frequency changes with changing inductance of the machine phase B. The tank is designed such that the resonant frequency moves closer to the injection frequency in regions where $\hat{u}_{\text{AC}}$ goes flat, increasing the injected current, thus increasing the sensitivity. It should be noted that current only increases when needed, avoiding unnecessary losses.

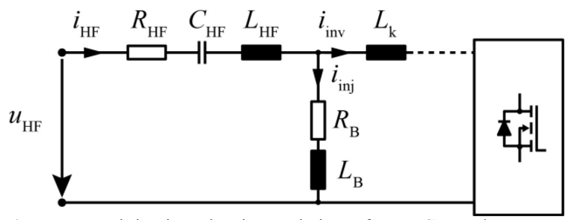

Figure 4. Resonant injection circuit consisting of R_{HF}, C_{HF} and L_{HF}. R_B and L_B are the resistance and the inductance of machine phase B, L_k is the motor side inductance of the LCL filter (not shown). The mutual couplings of machine phase inductances are not shown for the sake of simplicity.

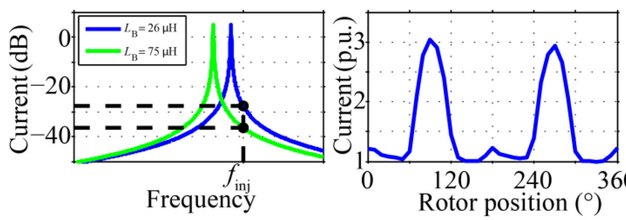

(a) (b)

Figure 5. (a) Injected current variation by changing resonant frequency of the injection LC tank. (b) Per unit values of the injected current for different rotor electrical positions.

C. Rotor Position Extraction

Firstly, u_{AC} is measured through blocking capacitors and a differential amplifier. It is then filtered using a band pass filter whose center frequency is set to the injection frequency. The band pass filter is constructed as a 4th order passive filter followed by an additional low pass filter, which is used to tune the phase if necessary. The differential measurement and the band pass filter are depicted in Figure 6.

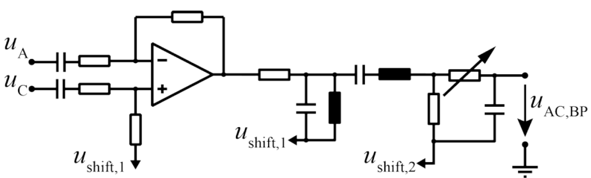

Figure 6. High frequency voltage measurement and filtering realized in hardware.

After the band pass filter, the signal $u_{AC,BP}$ needs to be demodulated to extract the rotor position information hidden in its amplitude. A well-known amplitude demodulation method is a simple multiplication of the signal with a cosine function of the same frequency, which can be explained as:

$$u_{sig} = \hat{u}_{sig}\cos(\omega_{sig}t), \tag{5}$$

$$u_{sig,DM} = \hat{u}_{sig}\cos(\omega_{sig}t)\cos(\omega_{sig}t), \tag{6}$$

$$u_{sig,DM} = \frac{\hat{u}_{sig}}{2} + \frac{\hat{u}_{sig}}{2}\cos(2\omega_{sig}t), \tag{7}$$

where u_{sig} is an amplitude modulated signal with angular frequency of ω_{sig} and $u_{sig,DM}$ is the demodulated signal. In (7), it is clear that multiplication with the carrier frequency moves the amplitude to DC and makes the further processing easier. In this work, a slightly different demodulation is implemented using analogue switches for a phase sensitive rectification (Figure 7). This means a

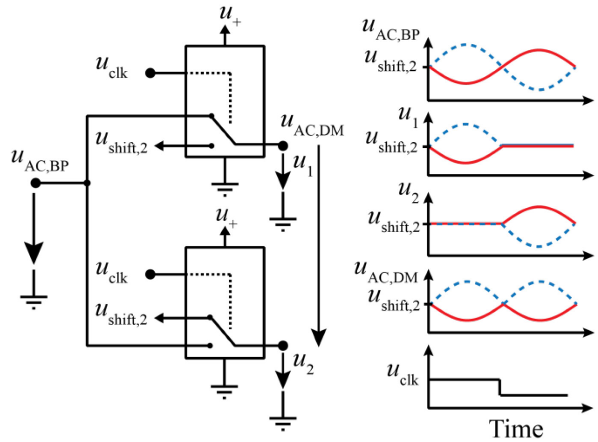

(a) (b)

Figure 7. (a) Phase sensitive rectification with analog switches. (b) Two different inputs and their respective rectification steps. Dashed blue line and solid red line show signals for two different rotor positions.

multiplication by a rectangular wave instead of a cosine function, yielding an average of $2\hat{u}_{sig}/\pi$ in the demodulated signal, which is higher compared to the $\hat{u}_{sig}/2$ in (7). The demodulated signal $u_{AC,DM}$ is obtained by using a differential amplifier circuit after the phase sensitive rectification.

Finally, the remaining demodulated disturbances are filtered out using a 4th order active low pass filter, built in Sallen-Key topology. The signal is then fed into the ADC of the DSP.

D. Initial Position Detection

It is clear on Figure 8 that the frequency of the signal fed into the ADC of the DSP is twice the electrical frequency of the rotor. This means that using this signal, the initial rotor position cannot be detected. However, in the example of the lateral stator machine, the saturation of the stator core can be used to determine the initial rotor position using well-known methods like the one presented in [6]. Furthermore, in most of the high speed applications, the machine is not required to start under load. For that reason, the initial position estimation is not considered any further in this paper.

E. Experimental Results

Figure 8 shows the digital rotor position signal (sampled by the ADC of the DSP) after the measurement, filtering and demodulation chain described above. It can be seen that almost the full range of the 12-bit ADC can be used for rotor position extraction, which proves the advantage of the differential measurement. It is also clear that the resonant injection tank helps to increase the sensitivity at the rotor positions where the signal goes flat.

The final estimation of the actual rotor position using the sampled ADC result can be achieved in different ways. A simple and accurate way is to store the waveform in an equidistance lookup table. However, this method may consume large amounts of DSP memory. Another approach may be to divide the waveform into linear regions and store only the starting point and the slope of the line. Figure 9 shows the results of the position estimation using lookup tables. Similar accuracy has also been achieved with the linear approximation method using considerably less memory; nevertheless it is not explained here due to space limitations.

III. CASE II: SLOTLESS PM MACHINE

A. Slotless PM Machine

As described in more detail in [1], the slotless PM machine, the machine of choice for many high speed applications, is a very low saliency machine with only a few percent impedance dependency on the rotor position because of the symmetrical rotor construction and lack of saturation in the stator core due to the large air gap. Furthermore, winding production methods generally introduce asymmetries in phase inductances, which are significant compared to the saliency. However, as explained above, with the help of differential measurements, even the slight saliencies can be measured accurately.

The slotless PM machine prototype used in this work is different than the lateral stator machine, not only because it is much less salient, but also because it does not have an accessible star point and because it has a titanium sleeve on its rotor. The lack of an open star point requires the modification of the signal injection approach used for the lateral stator machine. The titanium sleeve adds additional skin effect considerations and limits the signal injection frequency (otherwise any saliency coming from the rotor would not be visible). This makes the filter design more challenging as the injected sensing current and the drive currents cannot be separated from each other easily in the frequency domain.

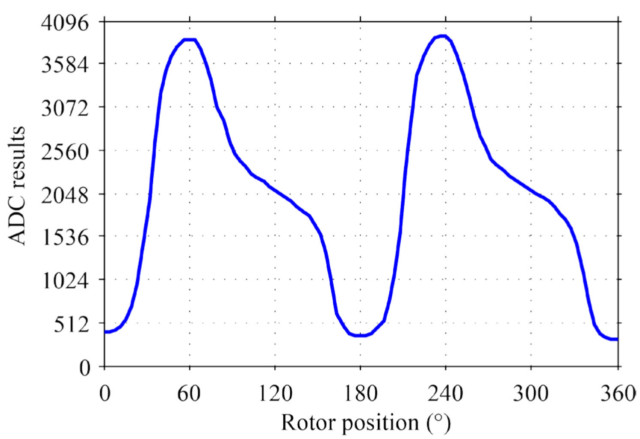

Figure 8. ADC results of the rotor position measurement. x-axis shows the rotor electrical position.

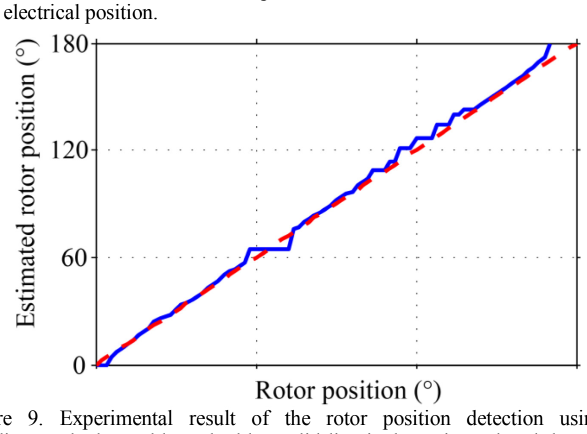

Figure 9. Experimental result of the rotor position detection using equidistance lookup tables. The blue solid line is the estimated and the red dotted line is the actual rotor position. Average rotor position estimation error is 2.3 degrees.

B. Proof of Concept - Simulation

The signal injection and differential measurement method for a slotless machine without star point connection is explained on the example that can be seen in Figure 10. A simple model is built using GeckoCIRCUITS circuit simulator software. A 5 V, 50 kHz voltage is applied to a PM machine with an extremely low (1%) saliency through the resistor R_{inj}, which limits the injection current. The difference of the currents through shunt resistors R_{s1} and R_{s2} are measured and plotted as well as the injection current. The simulation is repeated for different rotor positions at standstill. The results are plotted in Figure 11, where it can be seen that the difference of the currents through R_{s1} and R_{s2} (from now on to be called the differential current) depends on the rotor position. One way of extracting the rotor position from the differential current is sampling it at a certain time, for example at sampling instants shown by red arrows in Figure 11. The results of this sampling are shown in Figure 12. It has to be noted that, this waveform has zero offset, which means even the slightest saliencies (1% in this example) can be captured with high sensitivity, i.e., using the full scale of the ADC. It is also clear that the measured waveform has twice the electrical fundamental frequency, meaning that this is a relative position measurement and cannot be used to estimate the initial rotor position.

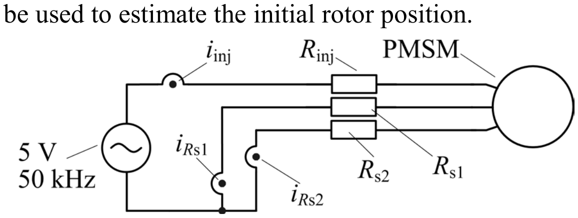

Figure 10. Simulation model used to explain the concept.

C. Proof of Concept - Measurements

The analysis described above is verified on two commercial slotless PM machines. Table I summarizes important properties of these two machines. First, the inductances of those machines are measured across their terminals using an impedance analyzer for different rotor positions at standstill. The results are shown in Figure 13.

Afterwards, an off-the-shelf signal generator and a power amplifier are used to inject a high frequency current into the machines, and two current probes are used to measure the injected and differential currents as shown in Figure 14, as described in [12]. The measurements are repeated at different rotor positions at standstill. The results for the

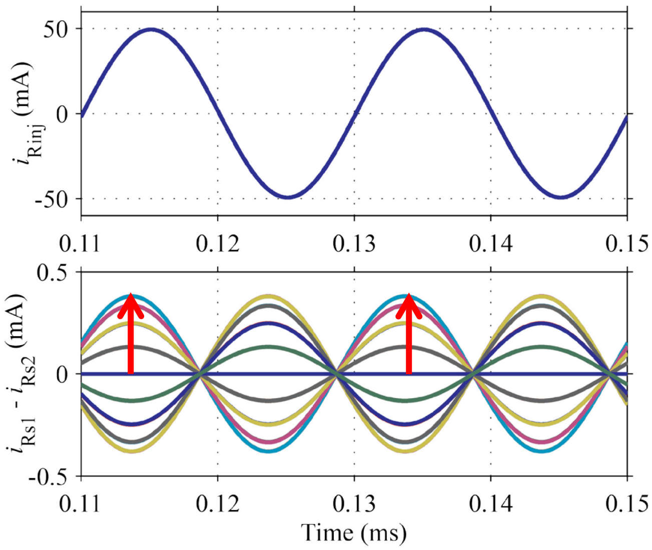

Figure 11. Results of the GeckoCIRCUITS model. Different colors represent different rotor positions. Red arrows denote the sampling instants for the next figure.

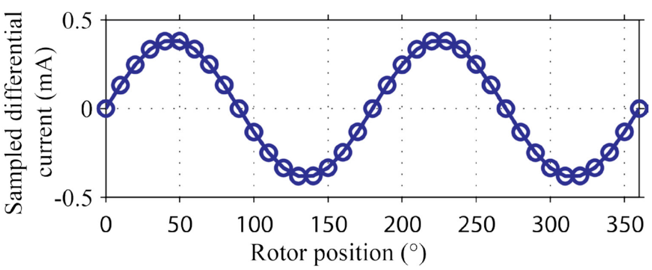

Figure 12. Differential current sampled at a certain time for all the different rotor positions.

TABLE I

	Tested slotless PM machines	
	Machine 1	***Machine 2***
Rated speed (rpm)	500,000	32,200
Rated power (W)	100	40
Numer of poles	2	2
Flux linkage (mWb)	0.75	5.3
Phase inductance (µH)	See Figure 13	See Figure 13
Producer / model	Celeroton / CM-2-500	Maxon / EC-22

machine 1 are shown in Figure 15 for 50 kHz injection and in Figure 16 for 300 kHz injection. Figure 17 shows the results for the machine 2 for 200 kHz injection.

It can be seen that the amplitude of the differential current in Figure 15 does not swing between a positive and a negative value depending on the rotor position like in Figure 11. Instead, it changes within a narrower range. This is due to the winding asymmetries introduced by the winding production method. This phenomenon decreases the sensitivity of the measurement system compared to the ideal case of Figure 11; however, the detectable change in the measurement signal is still around 50% which is much higher compared to that of the state-of-the-art inductance tracking methods where the current and/or voltage sensors would be required to detect the 2.5% saliency of the machine. This improvement of the sensitivity is an important advantage of using differential measurements.

The results of the same machine with higher injection frequency (300 kHz) are shown in Figure 16. The comparison of Figure 15 and Figure 16 reveals that increasing the injection frequency decreases the sensitivity of the measurement. This, as explained above, is due to the skin effect, which stops the fields from penetrating through the rotor at higher frequencies.

Figure 17 shows the results of the same measurement for the machine 2. It is clear that the winding asymmetries are not as strong in this machine.

It has been shown that even with the winding asymmetries of machine 1, the proposed method can increase the sensitivity of the rotor position estimation. However, in the next section the combination of the proposed method and the drive inverter will be explained on an example with the machine 2 and the winding asymmetries will be neglected for the sake of simplicity.

D. Combination of the Signal Injection, Differential Measurement and the Drive Inverter

In this section of this paper, the combination of the proposed signal injection and differential measurement method with the drive inverter is explained using an example. General guidelines for the design procedure are discussed and a complete simulation model is built in GeckoCIRCUITS to prove the applicability.

Figure 18 shows part of the simulation model of the drive inverter and the additional signal injection circuit. A standard voltage source inverter operating under space vector modulation is assumed to be driving the machine. The input voltage is constant at 100 V. The switching frequency fixed at 50 kHz.

The machine is modeled using an idealized PM synchronous model, where the winding asymmetries as well as saturation and skin depth effects are neglected. The electrical parameters of the machine such as the winding inductances and the flux linkage are set to represent machine 2.

An LCL filter is used between the inverter and the machine mainly for two reasons: damping the higher order harmonics in the drive current, and guiding the injected position detection current into the machine.

The LCL filters in such applications are usually associated with additional losses in the filter, additional cost and additional space requirements. However, in a very recent work [13] the losses in high speed drive systems are analyzed and the effect of the higher order harmonics especially on the rotor losses are pointed out. Under the light of that work, LCL filters can be considered as an opportunity for shifting the losses from the rotor of the

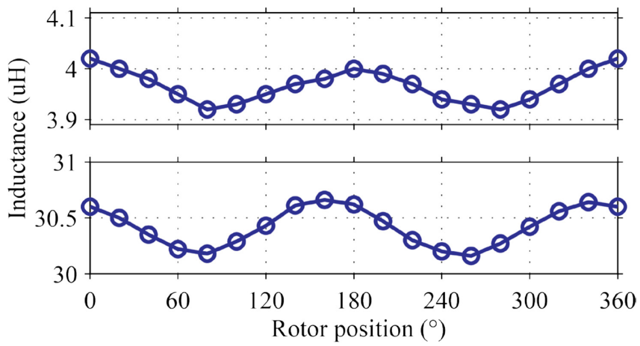

Figure 13. The inductances of machine 1 measured at 50 kHz (above) and machine 2 measured at 200 kHz (below). Calculated saliencies are 2.5% and 1.6%, respectively.

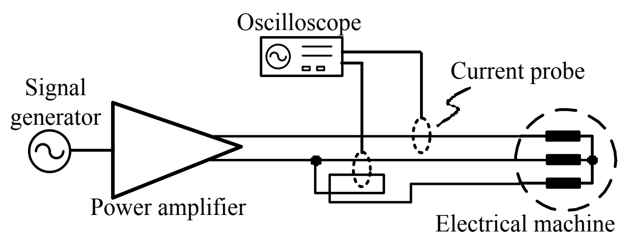

Figure 14. Test setup for the modified signal injection approach.

machine to the filter which generally has better cooling options.

L_f, L_k and C_f are chosen as 100 µH, 100 µH and 0.6 µF in order to set the resonance frequency to 40 kHz and damp the switching frequency harmonics by around -30 dB. The Bode plot of system is shown in Figure 19. The resonance frequency of the filter is set as a compromise between additional passive element size requirements, control bandwidth and filtering performance at the injection frequency.

The additional signal injection circuit is placed between the filter and the machine. A high frequency voltage is applied to the machine terminals in similar way of the test setup of Figure 14, through decoupling capacitors C_{hp}. The injection voltage is assumed to be of sinusoidal form, with amplitude of 5 V and a frequency of 175 kHz. The frequency is set such that it is sufficiently high for the LCL filter to show its effect, between two harmonic groups and lower than the skin effect related upper limit for that machine (several hundred kHz). In this configuration, around 75% of the injection current goes into the machine while the rest flows through the LCL filter elements. The current difference is measured using a differentially wound current transformer as proposed in [14] and [15]. In such a configuration, the current transformer can be dimensioned very small as it only carries the flux of the current difference, and small amount of leaking high frequency components of the drive current.

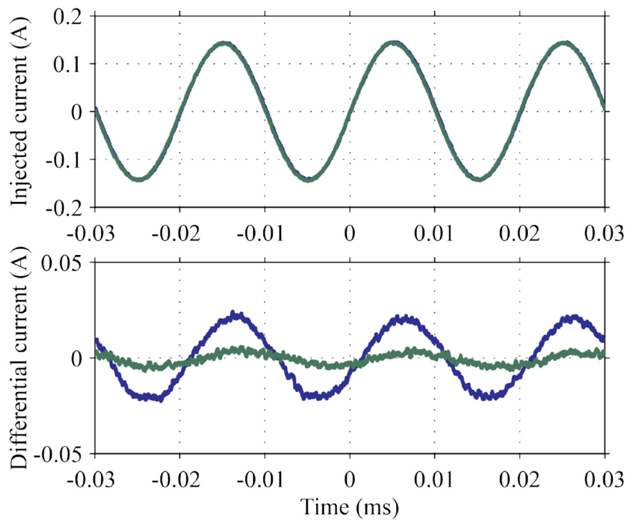

Figure 15. Measurement results of the 50 kHz signal injection on the machine 1. 90 degrees (blue), 0 degrees (green).

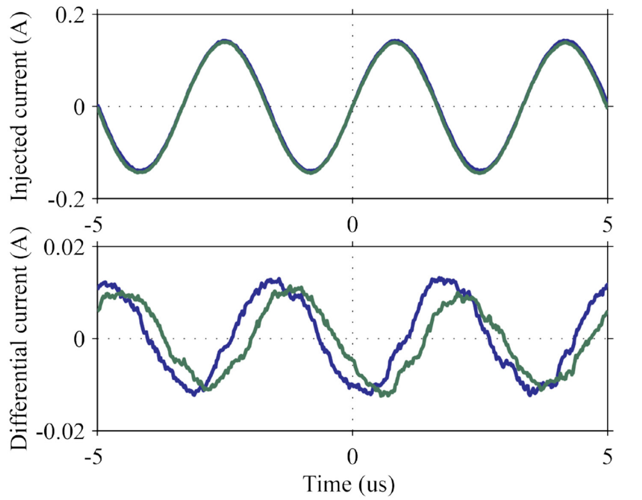

Figure 16. Measurement results of the 300 kHz signal injection on the machine 1. 90 degrees (blue), 0 degrees (green).

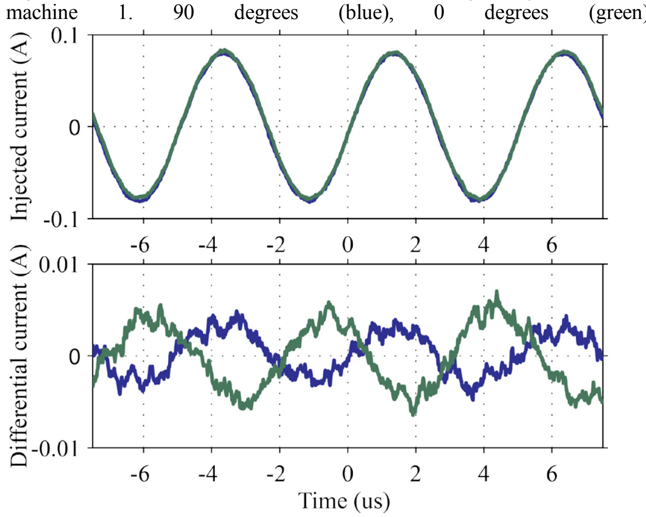

Figure 17. Measurement results of the 200 kHz signal injection on the machine 2. 90 degrees (blue), 0 degrees (green).

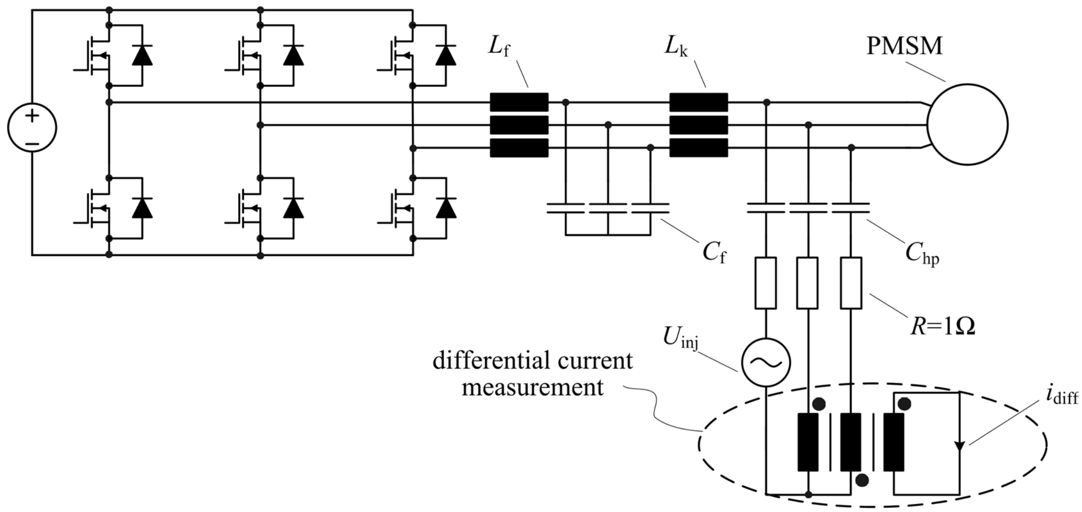

Figure 18. The drive system including the inverter, LCL filter additional signal injection and differential current measurement circuitry and the machine.

The skin effect related higher limit on the injection frequency makes the filtering more difficult, as the injection frequency and the drive harmonics cannot be placed far away from each other on the frequency domain. However, the low injection frequencies make it possible to use different filter applications such as switched capacitor or high accuracy active filter ICs for better practical filter realizations. For this work, a 4th order active band pass filter is designed using the FilterCAD and LTspice software from Linear Technology. This filter can be realized using the low noise filter IC LTC1562-2 and a few additional resistors. Once the filter is designed, its performance is mimicked in GeckoCIRCUITS using its transfer function. Figure 19 shows the Bode plot of the filter's transfer function.

The theory and the practical realization of amplitude demodulation are explained in detail in the first part of this paper. Here, for simplicity, only a multiplication with a sinus function is used for demodulation. Finally, a 4th order low pass filter which also modeled in the same way as the band pass filter is used to filter out the remaining components of the signal. The resulting signal is an offset free sinus, which has twice the frequency of the rotor's electrical position.

The simulation results show that a clean and offset free signal can be extracted from the measurements. This signal is in a sinusoidal shape and has twice the electrical frequency of the rotor. For that reason, a second measurement channel is required to have direction information. This can be realized by adding a second injector circuit or having one injector circuit and switching between the machine phases as described in [16] .

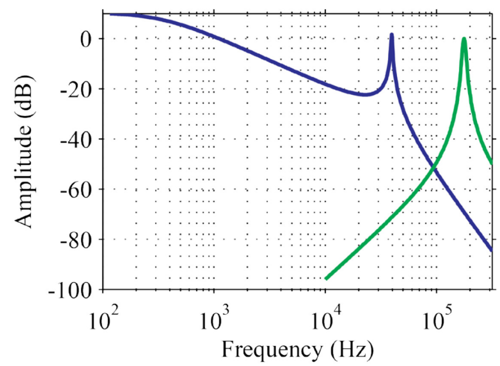

Figure 19. Bode magnitude plot of the relationship between the inverter output voltage to machine current (blue) and between band pass filter input and output (green).

IV. Conclusions and Outlook

A signal injection method to track the impedance change of an electrical machine and estimate the rotor position is proposed in this paper. The signal is injected using an additional circuit, decoupling the signal injection from the drive inverter. This avoids any need to alter the drive PWM modulation scheme or to increase the switching frequency. Differential measurements are used to measure the response of the machine, which makes it possible to use this method even for very low saliency machines. Finally, various steps of filtering and demodulation are constructed in analog hardware, reducing the computational effort of the DSP. All these features present an important step towards a practical full speed range self-sensing control of low saliency high speed machines.

Using the proposed self-sensing method, the position sensors in the machine can be omitted. This is in good agreement with the miniaturization trend in recent electrical

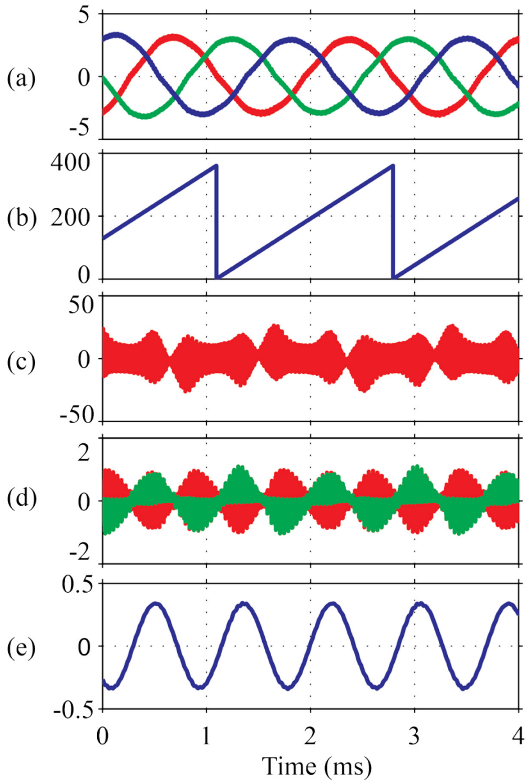

Figure 20. Simulation results for the slotless machine, operating at rated speed and power. (a) Machine phase currents in A. (b) Rotor position in electrical degrees. (c) Measured differential current in mA (assuming 1:1:1 turns ration on the differential current transformer). (d) Differential current after band pass filter (red) and demodulation (green). (e) Offset free signal containing rotor position information (in mV, if one to one current to voltage conversion is assumed).

drives, as even though the additional electronic components of the self-sensing method may be using larger space compared to the position sensors; they are placed on the inverter and not in the motor where the space limitation is an issue.

Two different applications of the proposed method are shown, on two different machine topologies. The effect of a conducting sleeve on the rotor, which is typical for high speed machines, is discussed along with that of the star point access. The applicability of the proposed method is demonstrated using measurement results on the lateral stator machine and comprehensive simulation results for the slotless PM machine.

Future work includes the enhancement of the method by adding a second measurement channel as described above, as well as experimental verification and dynamic load tests.

References

[1] J. Luomi, C.Zwyssig, A. Looser, and J. W. Kolar, “Efficiency optimization of a 100-W 500 000-r/min permanent-magnet machine including air-friction losses,” IEEE. Trans. on Ind. Appl., vol. 45, no. 4, Jul./Aug. 2009.

[2] A. Tüysüz, A. Looser, C. Zwyssig, and J.W. Kolar, “Novel miniature motors with lateral stator for a wide torque and speed range,” 36th Ann. Conf. of Ind. Electronics, IECON, pp. 1741-1747, Nov. 2010.

[3] C. Zwyssig, S. D. Round, and J. W. Kolar, “An ultra-high-speed, low power electrical drive system,” IEEE Trans. on Ind. Electron., vol. 55, no. 2, pp. 577 - 585, Feb. 2008.

[4] P.D. Pfister and Y. Perriard, “A 200 000 rpm. 2 kW slotless permanent magnet motor,” IEEE Int. Conf. on. Electrical Machines and Systems, pp. 3054-3059, Oct. 2008.

[5] S-C. Yang and R. D. Lorenz, “Comparison of resistance-based and inductance-based self-sensing control for surface permanent magnet machine using high frequency signal injection," IEEE Energy Conv. Cong. and Exp., ECCE, pp. 2701-2708, Sep. 2011.

[6] M. Schroedl, “Sensorless control of AC machines at low speed and standstill based on the INFORM Method,” 31th IAS Annual Meeting, Vol. 1, pp. 270-277, Oct. 1996.

[7] E. Robeischl and M. Schroedl, “Optimized INFORM measurement sequence for sensorless PM synchronous motor drives with respect to minimum current distortion,” IEEE Trans. on Ind. Appl., vol. 40, no. 2, pp. 591-598, Mar./Apr. 2004.

[8] T. M. Wolbank and J. Machl, “A modified PWM scheme in order to obtain spatial information of AC machines without mechanical sensor,” Appl. Power Electronics Conf. and Expo., vol. 1, pp. 310-315, 2002.

[9] H. Kim and R.D. Lorenz, “Carrier signal injection based sensorless control methods for IPM synchronous machine drives," 39th IEEE Ind. Appl. Conf., vol. 2, pp. 977- 984, Oct. 2004.

[10] D. Raca, P. Garcia, D.D. Reigosa, F. Briz, and R.D. Lorenz, “Carrier-signal selection for sensorless control of PM synchronous machines at zero and very low speeds,” IEEE Trans. on Ind. Appl., vol.46, no.1, pp.167-178, Jan./Feb. 2010.

[11] A. Tüysüz, D. Koller, A. Looser, and J.W. Kolar, “Design of a test bench for a lateral stator electrical machine,” 37th Ann. Conf. of Ind. Electronics, IECON, pp. 1736-1741, Nov. 2011.

[12] R. Leidhold and P. Mutschler, “Injection of a carrier with higher than the PWM frequency for sensorless position detection in PM synchronous motors,” 13th Power Elect. and Motion Control Conf.. EPE-PEMC, pp. 1353-1358, Sep. 2008.

[13] L. Schwager, A. Tüysüz, C. Zwyssig, and J.W. Kolar, “Modeling and Comparison of Machine and Converter Losses for PWM and PAM in High-Speed Drives,” to be published Int. Conf. on Elect. Mach. , ICEM, Sep. 2012.

[14] A. Looser and J.W. Kolar, “A hybrid bearing concept for high-speed applications employing aerodynamic gas-bearings and a self-sensing active magnetic damper,” 37th Ann. Conf. of Ind. Electronics, IECON, pp. 1686-1691, Nov. 2011.

[15] R. Leidhold and P. Mutschler, “Sensorless position detection in PM synchronous motors by injecting a high-frequency zero-sequence carrier,” 13th Europeean Conf. on Power Elect. and Appl., pp. 1-10, Sep. 2009.

[16] Jean-Pierre Voillat. “Device for controlling an electric motor.” U.S. Patent 6 337 554 B1, Jan. 8th 2002.